Michener JK and Smolke CD

SUPPLEMENTARY INFORMATION

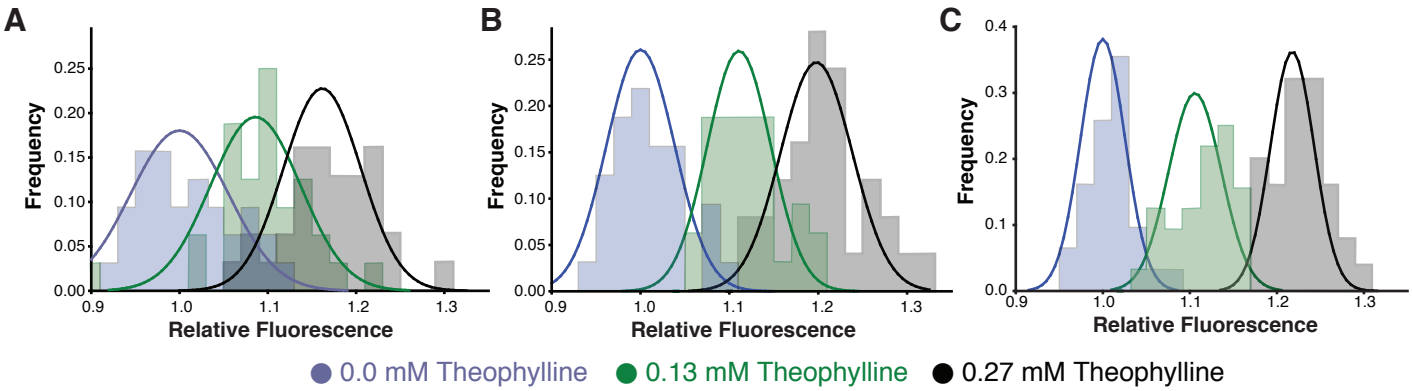

Supplementary Figure 1 Decreasing the cell-to-cell variation also decreases the culture-to-culture variation. When screening by flow cytometry, screening efficiency is determined by the coefficient of variation (CV) between replicate cultures. Expression noise within a single population affects the precision with which the mean can be determined and therefore the CV. For each of the screening constructs shown in Figure 2 (A: plasmid-GAL, B: plasmid-TEF, C: integrated-TEF), replicate cultures (n=32) were grown in the presence of varying amounts of theophylline and the geometric mean fluorescence of each culture was determined by flow cytometry. The relative fluorescence is the ratio of the geometric mean fluorescence for a single culture relative to the average geometric mean for all 32 uninduced cultures. The histograms show raw geometric means and the curves are fit to a normal distribution. The average CV of the three populations decreases from 5.0% (A) to 3.8% (B) and finally to 2.7% (C).

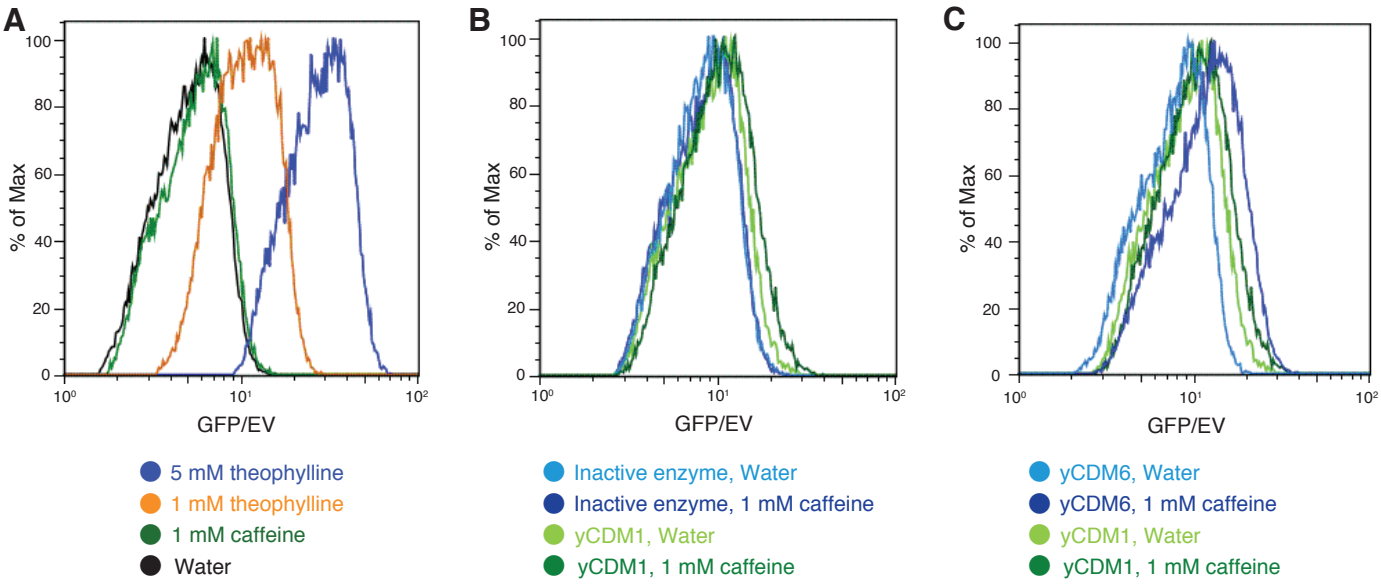

Supplementary Figure 2 One color fluorescence response histograms. (A) Fluorescence histogram of CSY492 grown in the presence of theophylline, caffeine, or water. The screening strain has a graded response to theophylline and no response to caffeine. (B) Fluorescence histograms of CSY492 containing active (green) and inactive (blue) versions of yCDM1. The fluorescence increases when caffeine is added to cells containing the active enzyme but is unchanged when caffeine is added to cells with the inactive enzyme. (C) Fluorescence histograms of CSY492 containing yCDM1 (green) and yCDM6 (blue). The more active enzyme produces a larger increase in fluorescence upon addition of caffeine.

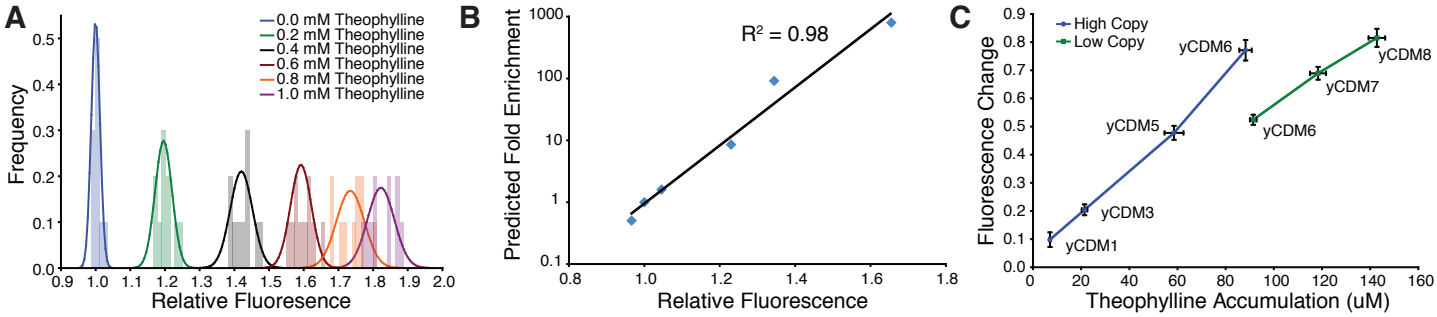

Supplementary Figure 3 Screening single cells by FACS is less sensitive than screening clonal cultures by flow cytometry. (A) When screening clonal cultures by flow cytometry, screening efficiency is determined by the coefficient of variation (CV) between replicate cultures. Replicate cultures of cells (n=10) containing the theophylline biosensor were grown in variable amounts of theophylline and analyzed by flow cytometry. The relative fluorescence is calculated as the ratio of the geometric mean fluorescence of a single culture to the average of the geometric mean fluorescence of all ten uninduced cultures. The histograms show raw geometric means, and the curves are fit to a normal distribution. The sensor has a CV of ~2.1%, allowing accurate discrimination of cultures with mean fluorescence differences of <10%. (B) When screening single cells by FACS, the efficiency is determined by the intrinsic noise within a population distribution relative to the difference in population means. Using our optimized sensor, the variation within a population is relatively constant, so the efficiency is strongly dependent on the ratio of fluorescence between the populations being separated. A switch with a larger dynamic range would improve the sorting efficiency, while additional intrinsic noise would reduce the efficiency. Cells containing the two-color screening system were grown in variable amounts of theophylline and analyzed by two-color flow cytometry. A representative sorting gate captured a small fraction of the uninduced cells (<0.1%) and increasing amounts of the more highly fluorescent populations. The ratio of these two percentages gives the predicted enrichment. The relative fluorescence is the ratio of the geometric mean fluorescence of the sample population to the geometric mean fluorescence of the uninduced control. The curve shown is an exponential fit to the experimental data. Screening single cells by FACS is highly effective when the changes in mean fluorescence are large, but this method cannot efficiently discriminate between small changes in mean fluorescence. (C) Improved enzymes produce more theophylline, which gives a larger fold activation of the RNA switch and, therefore, a better screening efficiency. Theophylline accumulation and switch activation are plotted for each of the enzymes described in this work. The fluorescence change is the increase in fluorescence of cells containing a given enzyme and grown with 1 mM caffeine relative to the same cells grown in the absence of caffeine ($[F_{caf}-F_{water}]/F_{water}$). The lines are a guide to the eye.

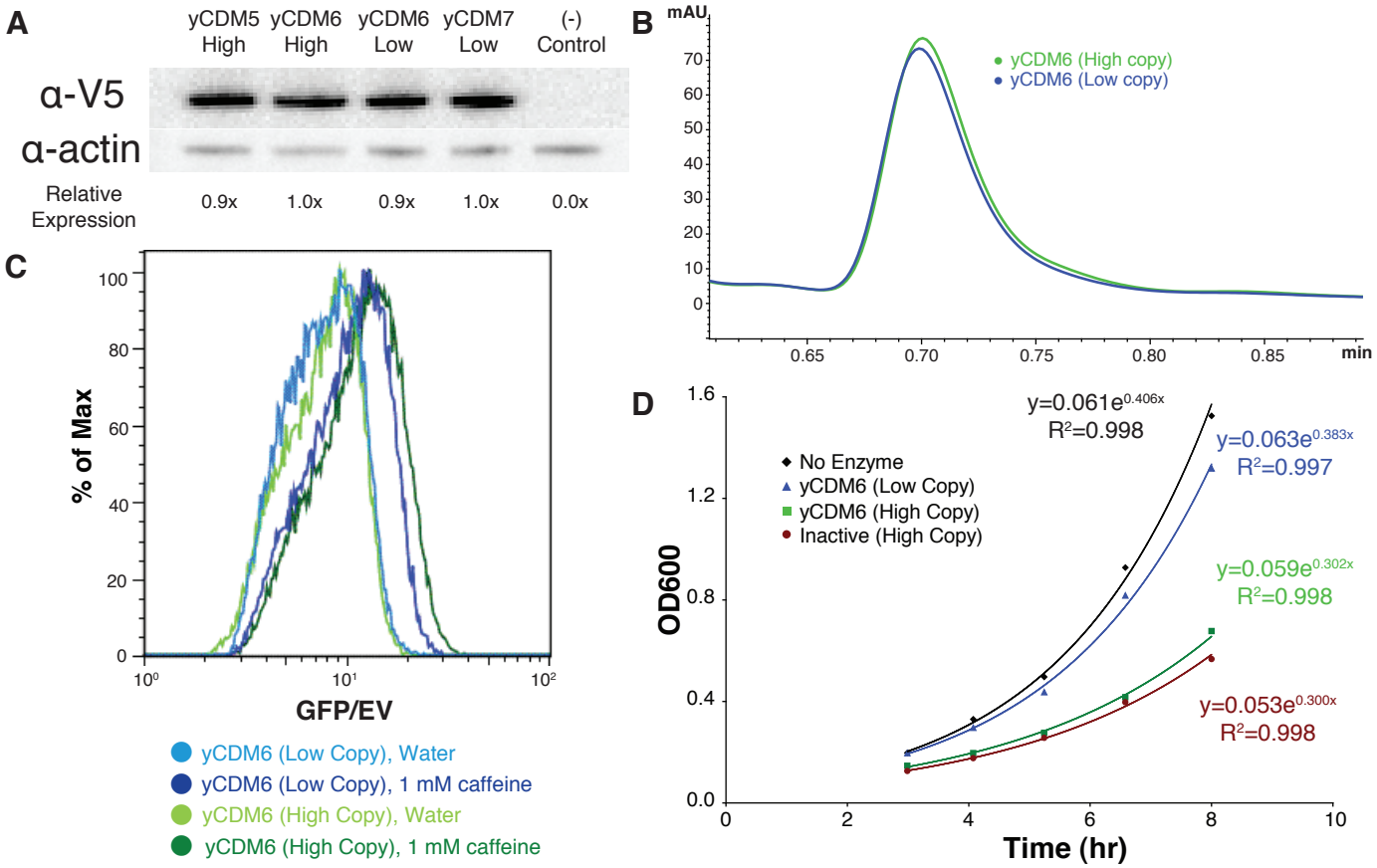

Supplementary Figure 4 Changing the plasmid copy number does not significantly affect enzymatic activity. (A) A Western blot demonstrates that total enzyme expression does not change as the DNA copy number is decreased. The enzyme contains a C-terminal V5 epitope, and the anti-actin antibody is used as a loading control. The relative expression values are calculated as the ratio of anti-V5 intensity/anti-actin intensity, normalized to yCDM6-High. The blot shown is representative of three independent experiments. (B) Total theophylline production differs by less than 10% between yCDM6-High (green) and yCDM6-Low (blue). Theophylline elutes at 0.70 minutes. (C) Fluorescence response histograms for yCDM6-High (green) and yCDM6-Low (blue). For each cell, the GFP fluorescence is normalized by the electronic volume (EV). Despite the similar levels of theophylline production, the low copy expression system shows a smaller change in fluorescence, presumably indicating lower theophylline per cell. (D) Growth curves for cells containing empty plasmid (black), yCDM6-High (green), yCDM6-Low (blue), or an inactive mutant (Neeli et al., 2005) of yCDM1 (brown). The curves are an exponential fit to the data. High-copy enzyme expression causes a significant decrease in growth rate. Lowering the plasmid copy number relieves ~80% of the growth inhibition. While the cells with the low expression system may produce less theophylline per cell, they grow faster and therefore have more time to make theophylline, resulting in similar total production.

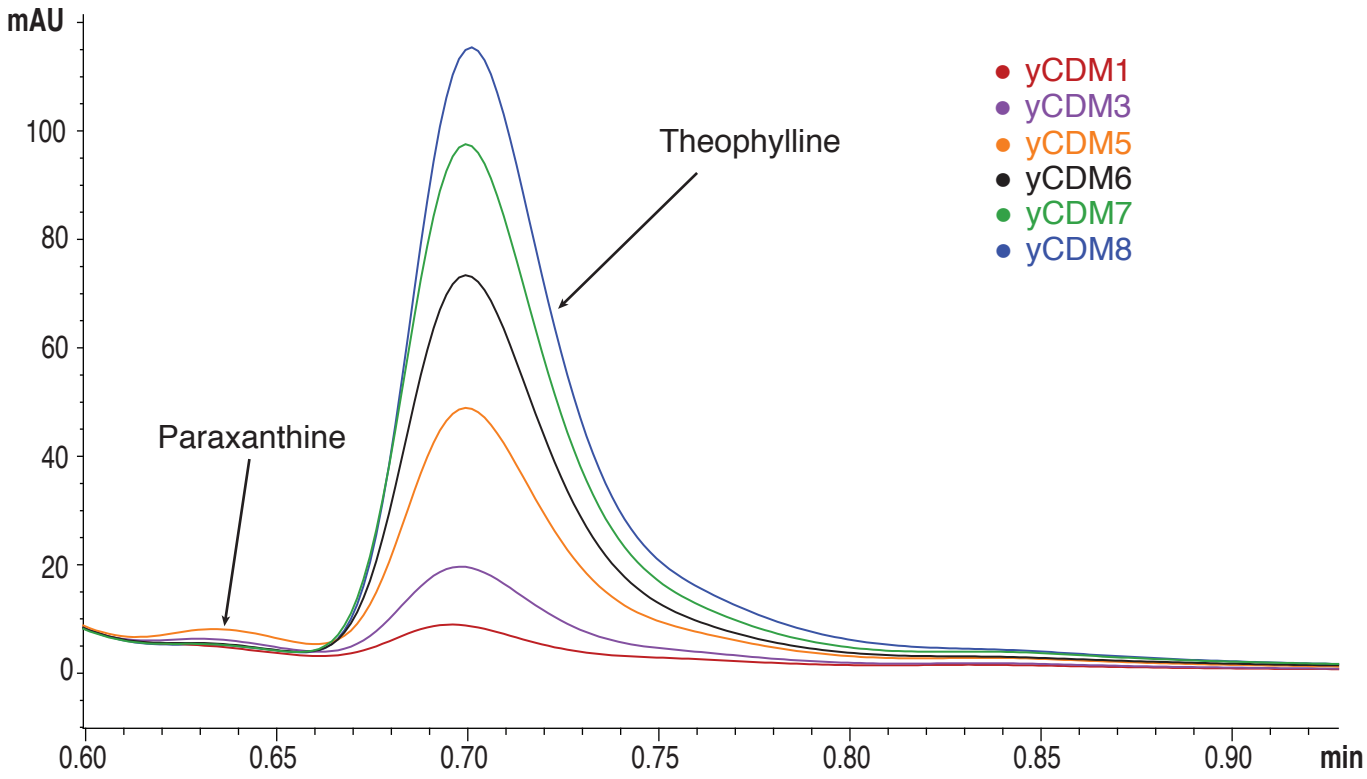

Supplementary Figure 5 Representative HPLC data. Cells containing each enzyme were grown in the presence of 1 mM caffeine. Culture supernatants were analyzed after 24 hours using HPLC analysis. Theophylline elutes at 0.70 minutes and paraxanthine elutes at 0.63 minutes.

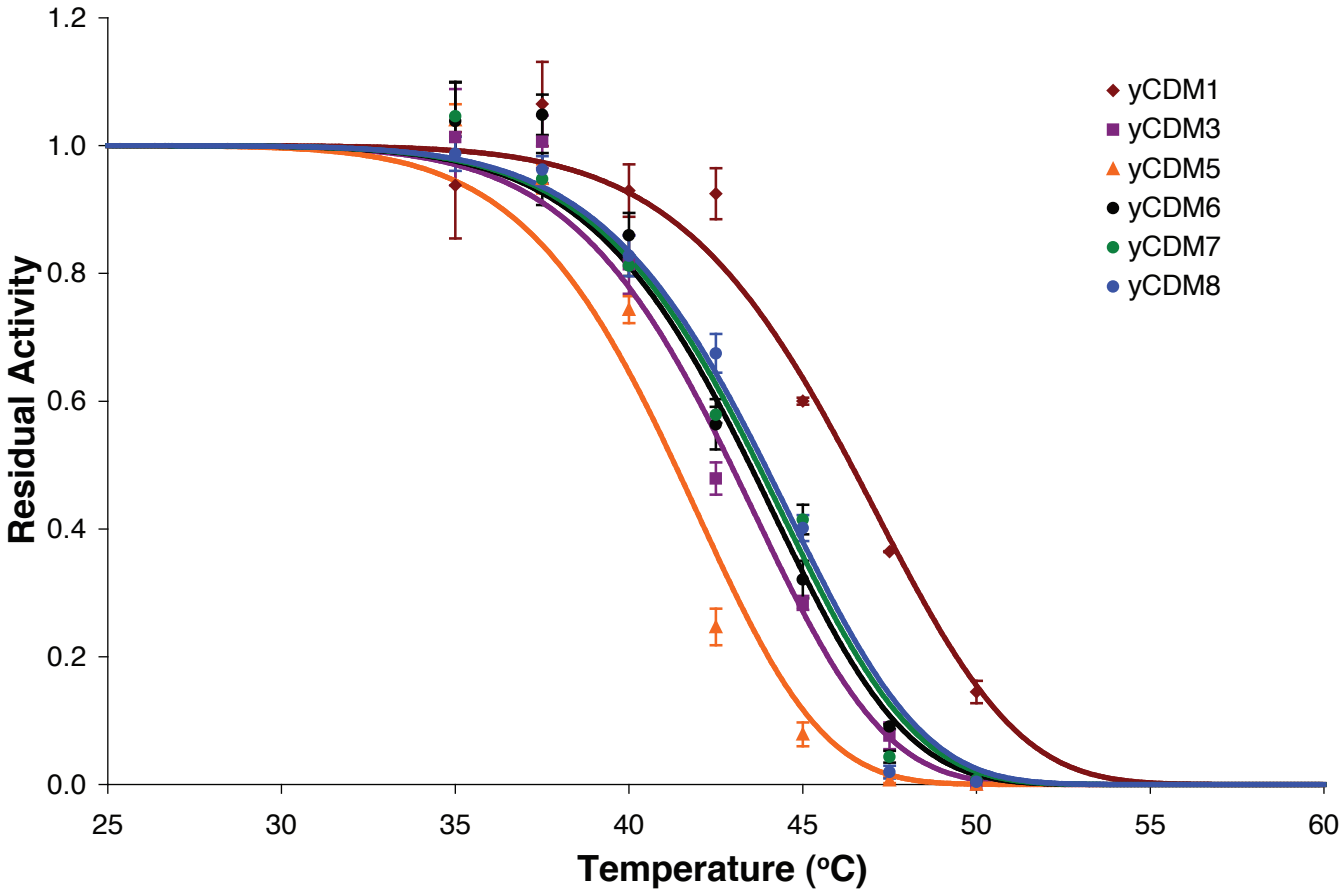

Supplementary Figure 6 Raw T_{50} curves. Crude E. coli lysate containing each enzyme was incubated for 10 minutes at the indicated temperature and then cooled on ice. 140 μL of enzyme was mixed with 20 μL of 20 mM NADPH and 40 μL of 25 mM caffeine. The residual theophylline production was measured by HPLC and normalized by the activity of lysate incubated at 4 °C. The data were fit to an Arrhenius inactivation curve, and the T_{50} was calculated as the temperature at which the fit showed 50% residual activity. The error bars show ± one standard deviation, calculated from three technical replicates. Note that these measurements for yCDM5 were an outlier, and replicate measurements did not show a statistically significant difference in T_{50} between yCDM3 through yCDM8.

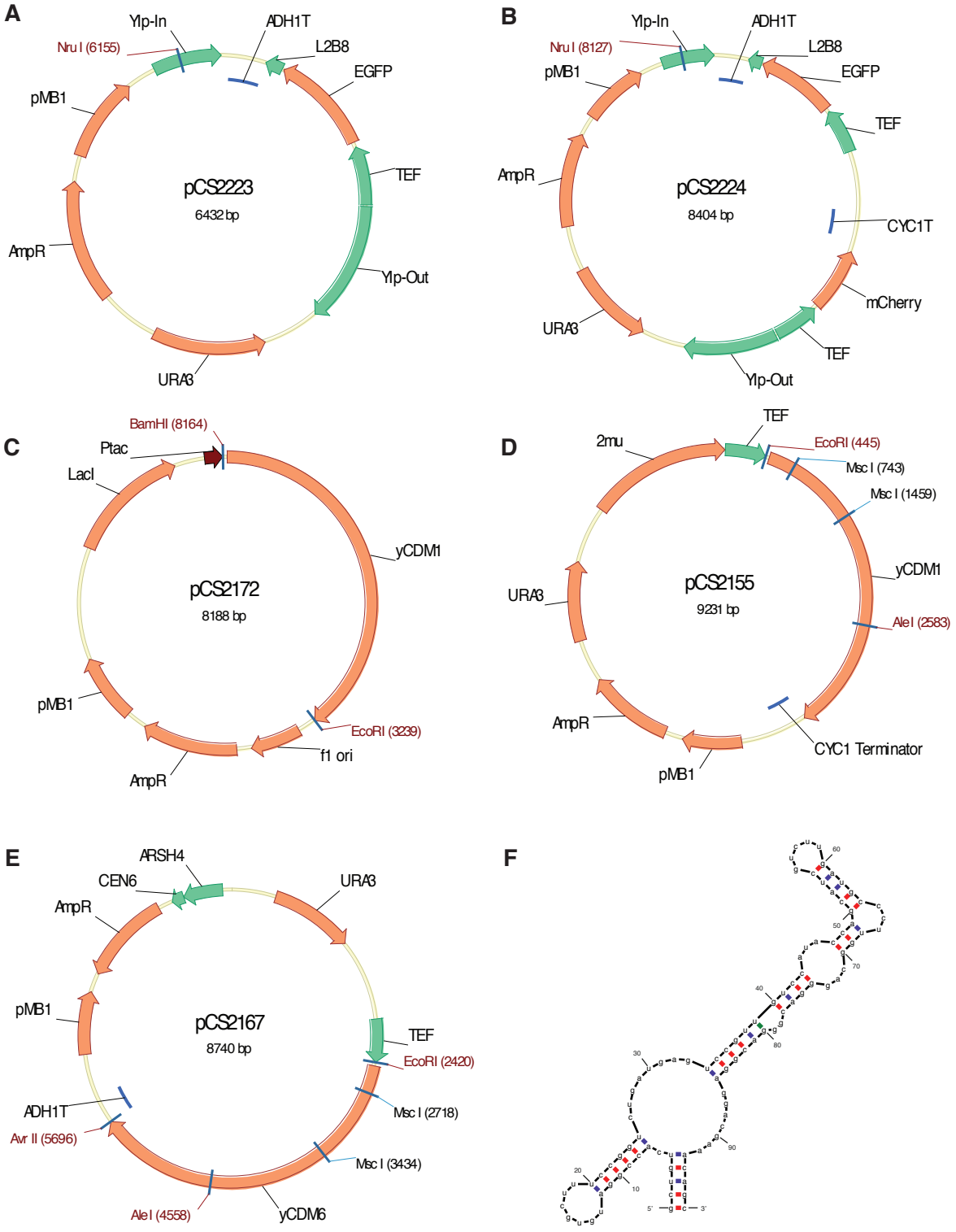

Supplementary Figure 7 Plasmid maps. (A) pCS2223, the single color integration vector used to construct CSY492. (B) pCS2224, the dual color integration vector used to construct CSY820. (C) pCS2172, the E. coli expression vector with yCDM1, used for T50 measurements. (D) pCS2155, the high copy yeast expression vector with yCDM1. (E) pCS2167, the low copy yeast expression vector with yCDM6. (F) The sequence and predicted structure of L2B8 (adapted from Win and Smolke, 2007).

Supplementary Table 1: Primers used in this study

Primer Name	**Primer Sequence**
BM3-FromWori-FWD	5’-TATAGAATTCGATATCAAGCTTGGAGATCTAAAAGAA AACAATGACAATTAAAGAAATGCCTCAG-3’
BM3-FromWori-REV	5’-CTATGCGGCCGCTCACCCAGCCCACACGTCTTTTG-3’
TEF-FWD	5’-ACTTCTTGCTCATTAGAAAGAAAGC-3’
yCDM-CEN-REV	5’-TATACCTAGGCTTCAATGGTGGTGGTGATGG-3’
yCDM-ToWori-FWD	5’-AATTGGATCCATCGATGCTTAGGAGGTCATATGTCTA TCAAAGAAATGCCAC-3’
yCDM-ToWori-REV	5’-TAATGAATTCTCAATGGTGGTGGTGATGGTG-3’
yMutF	5’-TCTTGCTCATTAGAAAGAAAGCATAGCAATCTAATC TAAGTTTTAATTAC-3’
yMutR	5’-AATCTAGCAGTAACTCTGTTGACGATACCTTCGTAGT TTCTTGGAATAAC-3’
30R	5’-CTTAAAGATTTCACCCAATTCGTCAGCAATTTTCATC-3’
30F	5’-GATGAAAATTGCTGACGAATTGGGTGAAATCTTTAAG-3’
60R	5’-CAAGTTCTTGTCGAATCTAGATTCATCACAAGCTTCC-3’
60F	5’-GGAAGCTTGTGATGAATCTAGATTCGACAAGAACTTG-3’
61R	5’-CAAGTTCTTGTCGAATCTAGATTCATCACAAGC-3’
61F	5’-GCTTGTGATGAATCTAGATTCGACAAGAACTTG-3’
85R	5’-CAGTTCTTTTCGTGGGTCCAGGAAGTGGCCAAACCG-3’
85F	5’-CGGTTTGGCCACTTCCTGGACCCACGAAAAGAACTG-3’
216R	5’-GGAGGCCTTTCTGTCAGCGATGATCTTGTCAAC-3’
216F	5’-GTTGACAAGATCATCGCTGACAGAAAGGCCTCC-3’
329R	5’-GTGTCTTCCTTAGCGTACAAAGAGAACCATGG-3’
329F	5’-CCATGGTTCTCTTTGTACGCTAAGGAAGACAC-3’
341R	5’-CACCCTTTTCCAATGGGTATTCACCACCCAAG-3’
341F	5’-CTTGGGTGGTGAATACCCATTGGAAAAGGGTG-3’
396R	5’-GCGAATTGTTGACCGATACAGGCTCTTTGACCG-3’
396F	5’-CGGTCAAAGAGCCTGTATCGGTCAACAATTCGC-3’

481R	5’-CCATGTTAGAACCGTACAAAACCAACAATG-3’
481F	5’-CATTGTTGGTTTTGTACGGTTCTAACATGG-3’
535R	5’-GCGTTATCTGCTGGATGACCGTTGTAGG-3’
535F	5’-CCTACAACGGTCATCCAGCAGATAACGC-3’
570R	5’-CCCAGTTTTTATCACCA-3’
570F	5’-TGGTGATAAAAACTGGG-3’
586R	5’-CACCCTTAGCAGCCAAAGTTTCGTC-3’
586F	5’-GACGAAACTTTGGCTGCTAAGGGTG-3’
663R	5’-CAATTCCTTGGAGGCAACGACGTTGGTAGAG-3’
663F	5’-CTCTACCAACGTCGTTGCCTCCAAGGAATTG-3’

Supplementary Table 2: Plasmids and strains constructed in this study

Strain	Genotype
W303	MATα *leu2-3,112 trp1-1 can1-100 ura3-1 ade2-1 his3-11,15*
CSY492	W303 *lys2::P_{TEF}-GFP-L2Bulge8-ADH1T*
CSY820	W303 *lys2:: P_{TEF}-mCherry-CYC1T-P_{TEF}-GFP-L2Bulge8-ADH1T*
pCS1423	Centromeric TRP P_{TEF}-GFP-L2Bulge8-ADH1T
pCS1767	Centromeric URA P_{GAL}-GFP-L2Bulge8-ADH1T
pCS2155	2µ URA P_{TEF}-yCDM1
pCS2156	2µ URA P_{TEF}-yCDM2a
pCS2157	2µ URA P_{TEF}-yCDM2b
pCS2158	2µ URA P_{TEF}-yCDM2c
pCS2159	2µ URA P_{TEF}-yCDM2d
pCS2160	2µ URA P_{TEF}-yCDM3
pCS2161	2µ URA P_{TEF}-yCDM4a
pCS2162	2µ URA P_{TEF}-yCDM4b
pCS2163	2µ URA P_{TEF}-yCDM4c
pCS2164	2µ URA P_{TEF}-yCDM4d
pCS2165	2µ URA P_{TEF}-yCDM5
pCS2166	2µ URA P_{TEF}-yCDM6
pCS2167	Centromeric URA P_{TEF}-yCDM6
pCS2168	Centromeric URA P_{TEF}-yCDM7
pCS2169	Centromeric URA P_{TEF}-yCDM8
pCS2170	2µ URA P_{TEF}-yCDM1 (A264H)
pCS2172	pCWori + yCDM1
pCS2173	pCWori + yCDM3
pCS2174	pCWori + yCDM5
pCS2175	pCWori + yCDM6
pCS2176	pCWori + yCDM7
pCS2177	pCWori + yCDM8
pCS2223	pIS385 + Centromeric URA P_{TEF}-yCDM6

pCS2224	pIS385 + P_{TEF}-mCherry-CYC1T-P_{TEF}-GFP-L2Bulge8-ADH1T
CSY821	CSY492+pCS2155
CSY822	CSY492+pCS2160
CSY823	CSY492+pCS2165
CSY824	CSY492+pCS2166
CSY825	CSY492+pCS2167
CSY826	CSY492+pCS2168
CSY827	CSY492+pCS2169
CSY828	CSY492+pCS2170
CSY829	CSY492+pCS2171
CSY830	CSY492+pCS4 (empty centromeric plasmid)
CSY831	CSY492+pCS31 (empty 2μ plasmid)
CSY845	W303+pCS1767
CSY846	W303+pCS1423

Supplementary Table 3: Mutations in the BM3 enzyme variants generated in this study

Enzyme	**Mutations**
yCDM1	A74W, V78I, A82L, F87A, M185V, L188W, A328F, A330W
yCDM2a	yCDM1 + I58T, P461L, A575V
yCDM2b	yCDM1 + N522S, C569Y
yCDM2c	yCDM1 + T22R, D194N, Q387R, A603T
yCDM2d	yCDM1 + S72F, P301L, G457D
yCDM3	yCDM1 + S72F, A603T
yCDM4a	yCDM3 + M354L, T576R, Q673K
yCDM4b	yCDM3 + F72I, T339I
yCDM4c	yCDM3 + R47S
yCDM4d	yCDM3 + Q27H, G660D
yCDM5	yCDM3 + Q27H, R47S, F72I
yCDM6	yCDM5 + E435G
yCDM7	yCDM6 + I174V
yCDM8	yCDM7+A87S

Supplementary Table 4: Summary of functional characterization data for enzyme variants

Enzyme	Relative $v_{max,\ app}/K_{M,\ app}$	$K_{M,\ app}$ (mM)	T_{50} (°C)	Selectivity
yCDM1	1.0	1.5 ±0.1	47.0 ± 0.6	10.3 ± 0.5
yCDM3	3.9 ±0.4	1.1 ±0.1	42.9 ± 0.9	14 ± 1
yCDM5	12.2 ±1.0	0.75 ±0.10	41.5 ± 1.3	23 ± 3
yCDM6	22.1 ±1.6	0.59 ±0.01	42.8 ± 1.0	100 ±25
yCDM7	26.6 ±3.1	0.74 ±0.02	42.1 ± 1.3	175 ± 4
yCDM8	33.0 ±4.2	0.69 ±0.04	43.1 ± 0.7	230 ±20